Molecular Biology of the Cell
Vol. 18, 4129–4142, October 2007

Rab6 Regulates Both ZW10/RINT-1– and Conserved Oligomeric Golgi Complex-dependent Golgi Trafficking and Homeostasis

Yi Sun, Anna Shestakova, Lauren Hunt, Siddharth Sehgal, Vladimir Lupashin, and Brian Storrie

Department of Physiology and Biophysics, University of Arkansas for Medical Sciences, Little Rock, AR 72205

Submitted January 29, 2007; Revised July 20, 2007; Accepted August 2, 2007
Monitoring Editor: Francis Barr

We used multiple approaches to investigate the role of Rab6 relative to Zeste White 10 (ZW10), a mitotic checkpoint protein implicated in Golgi/endoplasmic reticulum (ER) trafficking/transport, and conserved oligomeric Golgi (COG) complex, a putative tether in retrograde, intra-Golgi trafficking. ZW10 depletion resulted in a central, disconnected cluster of Golgi elements and inhibition of ERGIC53 and Golgi enzyme recycling to ER. Small interfering RNA (siRNA) against RINT-1, a protein linker between ZW10 and the ER soluble *N*-ethylmaleimide-sensitive factor attachment protein receptor, syntaxin 18, produced similar Golgi disruption. COG3 depletion fragmented the Golgi and produced vesicles; vesicle formation was unaffected by codepletion of ZW10 along with COG, suggesting ZW10 and COG act separately. Rab6 depletion did not significantly affect Golgi ribbon organization. Epistatic depletion of Rab6 inhibited the Golgi-disruptive effects of ZW10/RINT-1 siRNA or COG inactivation by siRNA or antibodies. Dominant-negative expression of guanosine diphosphate-Rab6 suppressed ZW10 knockdown induced-Golgi disruption. No cross-talk was observed between Rab6 and endosomal Rab5, and Rab6 depletion failed to suppress p115 (anterograde tether) knockdown-induced Golgi disruption. Dominant-negative expression of a C-terminal fragment of Bicaudal D, a linker between Rab6 and dynactin/dynein, suppressed ZW10, but not COG, knockdown-induced Golgi disruption. We conclude that Rab6 regulates distinct Golgi trafficking pathways involving two separate protein complexes: ZW10/RINT-1 and COG.

INTRODUCTION

How organelle homeostasis is maintained within the endomembrane system of eukaryotic cells is a paradigm-central question in cell biology. To grow and divide, eukaryotic cells must not only replicate their genomes but also the membranes of various organelles, including the nuclear envelope that delimits the nucleus and the plasma membrane that delimits the cell. Key to membrane replication is the endomembrane system within cells and the secretory pathway. The starting point of the secretory pathway is the endoplasmic reticulum (ER), from which newly synthesized proteins and lipids are transported to the Golgi apparatus, the central organelle of the secretory pathway. Within the Golgi apparatus, membrane components are modified, sorted, and transported to the plasma membrane, or, alternatively, to endosomes and lysosomes for expansion and replication of these essential organelles of the endomembrane system. In addition, there is a continuous and large-scale flux of cargo molecules (e.g., newly synthesized secreted proteins, internalized plasma membrane receptors, and/or recycling machinery proteins) through the system. How the organelles and their specialized functional domains are maintained in the face of membrane continuities and the flux of proteins through the endomembrane system is a major unanswered question. In particular, the molecular mechanism(s) by which organelle homeostasis is maintained for the mammalian Golgi apparatus (also known as the Golgi complex) are poorly understood (for reviews, see Shorter and Warren, 2002; Lee *et al*., 2004).

Golgi homeostasis may be considered both in terms of the overall organization of the organelle and as the balance of protein distributions between Golgi subcompartments and the ER. In mammalian cells, the Golgi apparatus is organized into a juxtanuclear ribbon of interconnected Golgi cisternal stacks. This is functionally important to protein sorting (Rogalski *et al*., 1984) and terminal glycosylation (Puthenveedu *et al*., 2006). Several lines of evidence suggest that maintenance of the Golgi ribbon is a balance among Golgi-associated motor activities, adherence of Golgi cisternal stacks to one another, and protein trafficking, all of which are under the control of members of the Rab family of small GTPase-timed molecular switches (for reviews, see Jordens *et al*., 2005; Short *et al*., 2005). For example, the Rab6 subfamily consisting of two closely related and likely functionally redundant isoforms, Rab6a and Rab6a′, expressed in all vertebrate cell types regulates recycling of Golgi enzymes to the ER by recruiting dynein-interacting effectors to Golgi membranes (Girod *et al*., 1999; Short *et al*., 2002; Matanis *et al*., 2003; Jiang and Storrie, 2005; Young *et al*., 2005; also see Del Nery *et al*., 2006 for an alternate viewpoint on the functional redundancy of Rab6a and Rab6a′). Rab1 and Rab2 interact with the golgin GM130, a coiled-coil protein important in holding the Golgi ribbon together (Allan *et al*., 2000; Weide *et al*., 2001; Puthenveedu *et al*., 2006). Other Rab effectors such as GRASP55, GRASP65, and golgin84 are important in adhesion of Golgi cisternae one to another into

This article was published online ahead of print in *MBC in Press* (http://www.molbiolcell.org/cgi/doi/10.1091/mbc.E07–01–0080) on August 15, 2007.

Address correspondence to: Brian Storrie (storriebrian@uams.edu).

a stack and for interlinking cisternal stacks into a Golgi ribbon (Short *et al.*, 2001; Diao *et al.*, 2003; Satoh *et al.*, 2003; Puthenveedu *et al.*, 2006). In addition, ER-to-Golgi and intra-Golgi trafficking seem to be essential to Golgi homeostasis. Depletion of p115, a coiled-coil protein thought to tether anterograde trafficking between the ER and Golgi apparatus, leads to fragmentation of the Golgi (Sohda *et al.*, 2005). p115 is a Rab1 effector (Allan *et al.*, 2000). Depletion of the Golgi-associated conserved oligomeric complex (COG) involved as a putative tether in intra-Golgi, retrograde trafficking, leads to fragmentation of the mammalian Golgi apparatus (Zolov *et al.*, 2005; Shestakova *et al.*, 2006). In yeast, at least two Rabs, Ypt1 and Ypt6, the homologue of mammalian Rab6, interact genetically with COG (Whyte and Munro, 2001; Ram *et al.*, 2002; Suvorova *et al.*, 2002). Furthermore, inhibition of protein exit from the ER causes the mammalian Golgi to redistribute into the ER (Storrie *et al.*, 1998). In yeast, Dsl1p and Tip20p likely form a tether complex for retrograde trafficking between the Golgi and ER that interacts with the soluble *N*-ethylmaleimide-sensitive factor attachment protein receptor (SNARE) Ufe1p (for reviews, see Lupashin and Sztul, 2005; Sztul and Lupashin, 2006). The mammalian homologues of Dsl1p, Tip20, and Ufe1p are ZW10 (see Supplemental Material in Andag and Schmitt, 2003), RINT-1 (Hirose *et al.*, 2004; Arasaki *et al.*, 2006) and syntaxin 18 (Hirose *et al.*, 2004), respectively.

Zeste White 10 (ZW10) was identified originally in *Drosophila* as a gene product required for normal segregation of mitotic chromosomes, and it is an evolutionarily conserved 82- to 89-kDa protein (Williams *et al.*, 1992; Starr *et al.*, 1997). In mitotic cells, it forms a molecular bridge between the kinetochore on chromosomes and components of the dynein motor complex. The presence of ZW10 is required for the Mad1/2 mitotic checkpoint linked to proper chromosome segregation (for review, see Karess, 2005). In interphase mammalian cells, ZW10 forms a complex with RINT-1 that binds to the ER SNARE syntaxin 18 (Hirose *et al.*, 2004; Arasaki *et al.*, 2006). Functionally, alteration of ZW10 interactions by antibodies, overexpression, and RNA interference had effects on the distribution of *cis*-Golgi markers and delayed the appearance of newly synthesized vesicular stomatitis virus-G protein at the plasma membrane (Hirose *et al.*, 2004). Whether ZW10 also directly interacts with the dynein motor complex in interphase cells is controversial. Hirose *et al.* (2004) tested for interactions between dynein and ZW10 in interphase HeLa cells and failed to find such interactions. In contrast, Varma *et al.* (2006) present evidence for decreased dynein recruitment to Golgi membranes with ZW10 knockdown and unbalanced motor activity as indicated by a greater decrease in minus- than plus-end–directed movements of Golgi elements and other organelles.

Here, we have focused on the role of Rab6 relative to ZW10/RINT-1 and the COG complex in Golgi trafficking/homeostasis in interphase mammalian cells. ZW10/RINT-1 and COG are putative retrograde tethers in Golgi-to-ER trafficking and intra-Golgi trafficking, respectively. Rab6 interference is a candidate suppressor of ZW10/COG loss-of-function–induced Golgi reorganization based of the known role of Rab6 in regulating retrograde trafficking (Martinez *et al.*, 1997; Girod *et al.*, 1999; White *et al.*, 1999). Our experimental results suggest that ZW10 has a role in retrograde trafficking of Golgi-associated proteins to the ER and in Golgi organization. More importantly, the data reveal a novel reciprocal relationship between Rab6 and ZW10 and its interacting partner RINT-1 in maintaining Golgi homeostasis. Furthermore, epistatic Rab6 loss-of-function specifically suppressed the dispersal of the Golgi ribbon associated with inactivation of COG. To the best of our knowledge, this is the first evidence that a Rab protein has a role in regulating Golgi membrane trafficking and homeostasis by affecting steps relative to two separate and distal protein complexes: ZW10/RINT-1 and COG.

MATERIALS AND METHODS

Cell Culture

HeLa cells stably expressing tagged Golgi apparatus proteins (GalNAcT2-GFP or GlcNAcT1-myc) were maintained in the presence of 0.45 mg/ml Geneticin (G-418 sulfate; Invitrogen, Carlsbad, CA). Cells were grown in DMEM supplemented with 10% fetal bovine serum in a humidified incubator at 37°C and 5% CO_2. All cell culture media and sera were obtained from Invitrogen. Cells were treated with brefeldin A (BFA) as described in Jiang *et al.* (2006).

RNA Interference (RNAi)

Dharmacon RNA Technologies (Lafayette, CO) manufactured all small interfering RNAs (siRNAs). The following siRNA sequences have been published previously: siZW10(102), siZW10(1911), siRINT-1(1149) by the Tagaya laboratory (Hirose *et al.*, 2004; Arasaki *et al.*, 2006); siCOG3 by the Lupashin laboratory (Zolov and Lupashin, 2005); siRNA directed against p115 (Sohda *et al.*, 2005), and siRab6a by the Goud laboratory (Del Nery *et al.*, 2006). The target sequence for siRab6(554) was 5′-GAGAAGAUAUGAUUGACAU-3′ with a UU overhang and that used for siRab5 was 5′-GCAAGCAAGUCCUAACAUU-3′ with a UU overhang. Control siRNAs were siCONTROL, nontargeting siRNA 1 (lot 050912). Duplexes were transfected at a final concentration of 200 nM, unless otherwise cited, by using Oligofectamine (Invitrogen) according to the manufacturer's protocol with minor revisions (Young *et al.*, 2005). Cells were transfected in the absence of fetal bovine serum. Typically after 72 h, cells were collected for Western blot or immunofluorescence staining. For double siRNA transfections, cells were transfected with a mixture of the siRNA duplexes with the concentration of each duplex at 100 or 200 nM as specified in the figure legends. In some cases, two cycles of siRNA experiments were done to achieve maximal knockdown (Young *et al.*, 2005). Cells were treated for the second time with the corresponding siRNAs after 60 h of transfection, and typically 12 h later, they were collected for analysis. No decrease in phenotypic penetrance was observed with incubations as long as 94 h postinitial transfection.

Antibodies

We affinity purified rabbit polyclonal antibodies directed against ZW10 by using a maltose binding protein (MBP)–ZW10 fusion protein (Starr *et al.*, 1997). Briefly, pMAL-HMG-ZW10 plasmid encoding MBP–HMG–ZW10 protein was expressed in TB1 bacteria. Bacteria were lysed, and MBP–HMG–ZW10 fusion protein was eluted from an amylose affinity chromatography column. The eluted MBP–HMG–ZW10 was electrophoresed, 10% SDS-polyacrylamide gel electrophoresis (PAGE), and transferred onto an enhanced chemiluminescence membrane (GE Healthcare, Little Chalfont, Buckinghamshire, United Kingdom). The region containing full-length ZW10 protein was cut out and incubated in phosphate-buffered saline (PBS)-Tween solution at 4°C overnight. The membrane was then incubated with PBS-Tween containing 5% bovine serum albumin for 1 h, washed three times with PBS-Tween, and then incubated in 0.2 M glycine buffer, pH 2.5, for 10 min to remove loosely bound proteins. After three washes with PBS-Tween, the membrane was incubated with 100-fold diluted anti-ZW10 crude antiserum for 2 h with slow rotation. After three washes, the bound antibodies were eluted from the membrane by incubation with glycine buffer for 2 min. Eluted antibody was neutralized immediately with 1.5 M Tris solution, pH 8.8, containing 5% bovine serum albumin and stored at −20°C. The crude rabbit anti-ZW10 antiserum and pMAL-HMG-ZW10 plasmids were gifts from Dr. Michael Goldberg (Cornell University, Ithaca, NY).

Affinity purified anti-COG3p was produced as described previously (Suvorova *et al.*, 2001). Mouse monoclonal anti-p115 was produced as described previously (Sapperstein *et al.*, 1995). Several antibodies were purchased commercially: rabbit anti-Rab6 (C-19 peptide) and goat anti-RINT-1 (N-15, C-15 peptides) were from Santa Cruz Biotechnology (Santa Cruz, CA); mouse antibodies directed against EEA1 (clone 14), GM130 (clone 35), Rab5, or GS27 were from BD Biosciences (San Jose, CA); mouse anti-glyceraldehyde 3-phosphate dehydrogenase (GAPDH) was from Ambion (Austin, TX); mouse anti-LAMP2 (clone H4B4) was from Developmental Studies Hybridoma Bank (University of Iowa, Iowa City, IA); mouse anti-GalT was from Cell Mab AB (Mönadl, Sweden); rabbit antibodies directed against the myc epitope tag were from Bethyl Laboratories (Montgomery, TX); rabbit anti-tubulin and mouse anti-actin were from Sigma-Aldrich (St. Louis, MO); and Cy3- or Cy5-conjugated donkey anti-mouse or anti-rabbit immunoglobulin (Ig)G antibodies were from Jackson ImmunoResearch Laboratories (West Grove, PA). Antibodies against GRASP55, GRASP65, protein disulfide isomerase, and Sec13a were gifts as described previously (Jiang *et al.*, 2006).

Microinjection

Wild type or GalNAcT2-GFP HeLa cells were grown on coverslips, and an Eppendorf microinjection system was used as described previously (Storrie, 2005b). Wild-type HeLa cells were microinjected with plasmids encoding tsO45-G protein conjugated to green fluorescent protein (GFP) as described in Jiang *et al*. (2006). Sar1p dominant-negative ER exit blocks were achieved by microinjection of pCMUIV plasmids encoding guanosine diphosphate (GDP)-restricted Sar1p as described previously (Stroud *et al*., 2003). Plasmids encoding Bicaudal D (BicD)-C fragment (60–100 ng/μl stock DNA concentration, pcDNA3.1myc A BicD2 [C-terminal amino acids 706–824]; Francis Barr, Max Planck Institute for Biochemistry, Martinsreid, Germany) or encoding GDP-Rab6a (100 ng/μl stock DNA concentration, Girod *et al*., 1999; Jiang and Storrie, 2005) were microinjected into the cell nucleus 48 h after ZW10 siRNA treatment. The expression period was 24-h expression. For anti-hCOG3 antibody microinjection, cells were microinjected in the cytoplasm 72 h after Rab6 siRNA treatment with affinity-purified anti-COG3 antibody (0.16 mg/ml stock concentration) or preimmune IgG (0.16 mg/ml). Cells were incubated at 37°C and 4 h postantibody injection fixed. In antibody microinjection, the coinjection marker was fixable Cascade blue dextran (Invitrogen) at a concentration 0.6 mg/ml.

Fluorescence Microscopy

Cells were grown on coverslips the day before transfection, and then typically 72 h after siRNA transfection, they were fixed and stained with appropriate antibodies as described previously (Jiang and Storrie, 2005; Shestakova *et al*., 2006). Widefield microscopy and imaging were performed with a Zeiss Axiovert 200M microscope (Carl Zeiss, Jena, Germany) fitted with high numerical aperture (0.80 or 1.4) 20, 63, and 100× objectives and a CARV II spinning disk confocal accessory (BD Bioimaging, Rockville, MD) mounted to the sideport of the microscope. Widefield images were taken with a CoolSnap HQ camera (Roper Scientific, Phoenix, AZ). Confocal images were captured to a Retiga EXi camera (Qlmaging, Burnaby, BC, Canada). Software control was with IPlab 3.9.5 Apple Macintosh version software (Scanalytics, Fairfax, VA). Image stacks for the Golgi apparatus collected through the entire cell depth were compressed into a single plane by using a maximum intensity projection and IPLab software. Deconvolution and image rendering was done with Huygens Essential software (SVI, Hilversum, The Netherlands). Images were additionally processed with Adobe Photoshop 7.0 software (Adobe Systems, Mountain View, CA). Matched images sets were mapped to a common gray scale range.

Fluorescence photobleaching was done with a Zeiss LSM510 Meta accessory mounted on a Zeiss 200M inverted microscope. A 63×/1.4 numerical aperture objective operated at 2.5× zoom was used, 0.11- × 0.11-μm XY pixel size. The confocal pinholes were at 4.17 Airy units. Cells were kept in Dulbecco's phosphate buffered saline containing calcium and magnesium and 2% fetal bovine serum. Photobleaching of GalNAcT2-GFP was done at room temperature, maximum power for the Argon laser, 488 nm laser line, 30 iterations, 2.5× zoom, ~1- × 1-μm^2 area, whereas images were collected with the laser power attenuated to 1% and averaged four times. Three images were collected before bleaching, 20 s apart, and postbleaching images were collected 20 s apart for almost 700 s. Zeiss software was used for microscope control and quantification of intensities.

Western Blot Analysis

HeLa cells were lysed in 2% SDS, followed by standard SDS-PAGE (~12% acrylamide) and Western blotting as described previously (Shestakova *et al*., 2006). Antibodies and dilutions used for Western blotting were anti-ZW10 (affinity purified, 1:100), anti-Rab6 (1:1000), anti-LAMP2 (1:100), anti-Rab5 (1:500), anti-RINT-1 (1:1000), anti-COG3 (1:1000), anti-p115 (1:500), anti-myc (1:5000), anti-actin (1:10,000), anti-α-tubulin (1:2000), and anti-GADPH (1:1000).

RESULTS

ZW10 Depletion Fragments the Golgi Ribbon to a Central Cluster of Golgi Elements

The initial experimental goal was to compare the effects of ZW10 and Rab6 knockdown on the organization of the Golgi ribbon and overall minus- and plus-end–directed motor activity in HeLa cells. To knockdown ZW10 and Rab6 protein levels, we took a siRNA approach by using siRNAs beginning at nucleotide 102 [siZW10(102)] and 1911 [siZW10(1911)] within the coding sequence of ZW10 mRNA and a siRNA beginning at nucleotide position 554 within the coding sequence of Rab6 [siRab6(554)]. The two ZW10 siRNAs are identical to those used by Hirose *et al*. (2004) and Varma *et al*. (2006). The Rab6 siRNA is directed against a 3′ portion of Rab6 mRNA that is common to both Rab6a and Rab6a′. By antibody staining, ZW10 is known to be a predominantly ER protein in interphase HeLa cells (Hirose *et al*., 2004; Kops *et al*., 2005; Varma *et al*., 2006). Rab6 is Golgi associated and concentrated in the *trans*-Golgi/*trans*-Golgi network (TGN; Antony *et al*., 1992).

As shown in Figure 1A, a 72-h treatment of HeLa cells with siZW10(102) or siRab6(554) resulted in a substantial knockdown of their respective proteins by immunoblotting. For ZW10, the observed knockdown was >80%. In agreement with Hirose *et al*. (2004) and Varma *et al*. (2006), we found that siZW10(1911) was less effective in depleting ZW10 protein levels (data not shown). For Rab6, the knockdown was >90% by immunoblotting. This knockdown must affect both Rab6a and Rab6a′ equally, because the two closely related proteins are present in equivalent amounts in HeLa cells, and they cannot be distinguished one from the other by the antibody used. We conclude that the siRab6(554) treatment effectively depleted both Rab6a and Rab6a′. Hence, we use the generic term Rab6 depletion/knockdown. Finally as demonstrated in Figure 1A, siRNA depletion of neither Rab6 nor ZW10 had little obvious effect on the processing of LAMP2, a lysosomal membrane protein, as indicated by the broad band expected for a highly glycosylated protein in immunoblots. In fact, if anything, as indicated by the slightly retarded migration of LAMP2 in the Rab6 siRNA case, glycosylation was promoted. As much of the processing of the oligosaccharide side chains of LAMP2 occurs in the cisternal stacks of the Golgi apparatus, we suggest that the Golgi, irrespective of any organizational consequences on the Golgi ribbon, must be, at least, basally functional.

Next, we determined the phenotypic effect of each siRNA treatment on the organization of the Golgi ribbon and the distribution of microtubules in HeLa cells (Figure 1, B–D). We chose to characterize microtubule distribution in the same cells because microtubules are the tracks on which microtubule-dependent transport of organelles/vesicles occurs and to give a counterstain to the Golgi apparatus that indicates the general dimensions of the cell. In all cases at 72 h, the distribution of microtubules (white) seemed similar in control (scrambled siRNA), siZW10(102)-treated cells, and in siRab6-treated cells, indicating both that the cells were healthy and that microtubules were available as normal for organelle transport.

As shown in Figure 1B, the normal distribution of the Golgi ribbon, as indicated by the distribution of the stably expressed, tagged, Golgi enzyme GalNAcT2-GFP was juxtanuclear with a relatively compact distribution that in some cells wraps around the nucleus (control: scrambled siRNA). With ZW10 depletion, cells displayed a clustered punctate distribution for GalNAcT2 (Figure 1C). Quantitatively, 95% of the siZW10(102)-treated cells displayed a clustered, punctate Golgi distribution at 72 h; only an occasional, nondisrupted Golgi ribbon was seen (Figure 1C, asterisk). Strong phenotypic penetrance was observed also at 48 h after transfection. The ZW10(102) knockdown phenotypic effect that we observed 72 h after transfection, although similar, was more pronounced than that seen by the Tagaya laboratory (Hirose *et al*., 2004; Arasaki *et al*., 2006). Similar to Hirose *et al*. (2004) and Varma *et al*. (2006), we found that siZW10(1911) produced a much less pronounced disruption of the Golgi ribbon (data not shown). In comparison, siRab6 treatment produced, if anything, a slightly more compact juxtanuclear Golgi ribbon (Figure 1D). This was decidedly more obvious in YZ projections of the confocal image stacks (data not shown). Using different siRNA-directed against a sequence

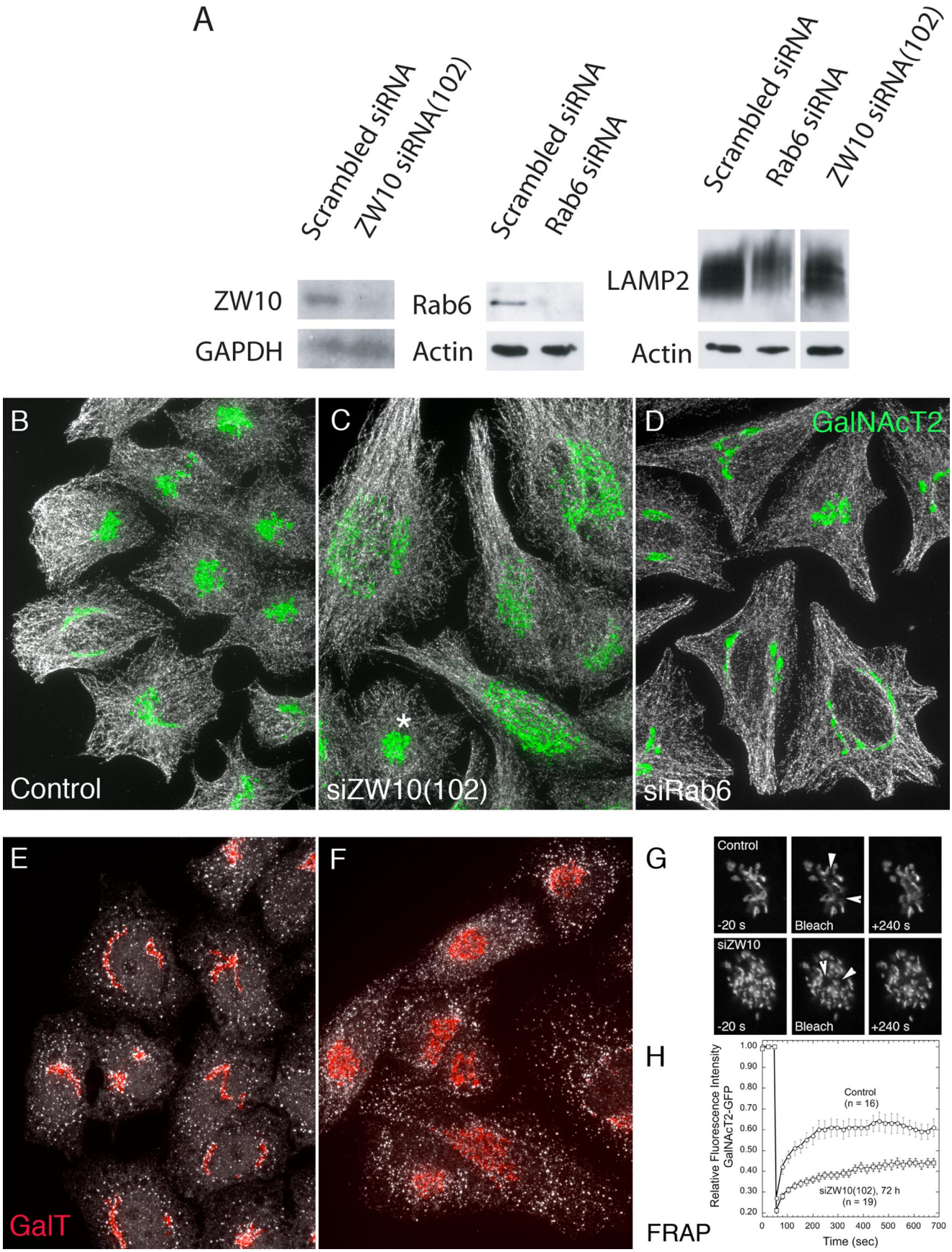
A
Scrambled siRNA
ZW10 siRNA(102)
Scrambled siRNA
Rab6 siRNA
Scrambled siRNA
Rab6 siRNA
ZW10 siRNA(102)
ZW10
GAPDH
Rab6
Actin
LAMP2
Actin
B
Control
C
siZW10(102)
D
GalNAcT2
siRab6
E
GalT
F
G
Control
-20 s
Bleach
+240 s
siZW10
-20 s
Bleach
+240 s
H
Relative Fluorescence Intensity GalNAcT2-GFP
Control (n = 16)
siZW10(102), 72 h (n = 19)
Time (sec)
FRAP

Figure 1.

common to both Rab6a and Rab6a′ mRNA, Nizak *et al*. (2003), Young *et al*. (2005), and Del Nery *et al*. (2006) also find that the Golgi ribbon can be more compact with Rab6 knockdown. Finally, we found the same Golgi phenotype was produced by cotransfecting cells with essentially the same siRNAs as Del Nery *et al*. (2006) use to selectively knockdown Rab6a and Rab6a′ (data not shown).

GalNAcT2-GFP is an overexpressed Golgi marker. Hence, we next characterized the distribution of endogenous β1,4-galactosyltransferase (GalT). As shown in Figure 1, E and F, when the distribution of GalT (red) was compared in control and ZW10 siRNA-treated cells, a similar effect on Golgi ribbon organization was observed. Depletion of ZW10, an ER-associated protein in HeLa cells (Hirose *et al*., 2004; our unpublished data), had little, if any, effect on the distribution or incidence of ER exit sites as indicated by punctate Sec13a staining (Figure 1, E and F, white) or on the distribution of ER luminal marker protein disulfide isomerase (data not shown). The centrally clustered Golgi elements induced by ZW10 depletion seem, at the light microscope level, similar to those induced by GM130 or GRASP65 depletion (Puthenveedu *et al*., 2006). These proteins are thought to be important to adherence of the Golgi ribbon. As shown by Puthenveedu *et al*. (2006), the centrally clustered Golgi elements in GM130- or GRASP65-depleted cells are separate from one another; in a fluorescence recovery after photobleaching (FRAP) assay, they act as if they are not connected together. In a similar set of FRAP experiments, we found that GalNAcT2-GFP fluorescence recovered rapidly after photobleaching in control cells (scrambled siRNA) but not in siZW10(102)-treated HeLa cells (Figure 1, G and H, arrowheads point to the photobleached regions). We conclude that there is little interconnection of Golgi elements in siZW10 HeLa cells. Note that our FRAP experiments were done at 24°C. Control FRAP recoveries are higher when done at 37°C (Puthenveedu *et al*., 2006). We also note here that by electron microscopy Hirose *et al*. (2004) find that the Golgi apparatus in siZW10(102) cells is a series of ministacks rather than as a continuous Golgi ribbon. With GM130 or GRASP65 knockdown, Puthenveedu *et al*. (2006) find that the sugar *N*-acetyl-D-glucosamine is more readily detected on the surface of cells, indicative of a glycosylation defect. Using the same lectin as Puthenveedu *et al*. (2006), we found no increase in *N*-acetyl-D-glucosamine exposure at the cell surface of ZW10-depleted cells (data not shown).

Although GalNAcT2 and GalT are excellent transmembrane markers for the Golgi ribbon, their distributions are not necessarily indicative of all Golgi proteins. Therefore, we examined the distribution of a number of other Golgi associated proteins with a particular concentration on endogenous golgins. As shown in Figure 2A, a central cluster of Golgi elements were noted in siZW10(102)-treated cells for the following proteins: kinesin, Rab6, GRASP55, GRASP65, p115, and GM130. For each, antibodies directed against endogenous proteins were used, confocal fluorescence image stacks were taken at the same exposure time, and the image stacks were projected into a single plane in the same manner for control (scrambled siRNA) and siZW10(102)-treated cells. The image intensities suggest that there was little to no decrease in the level of any of these proteins with siZW10(102) treatment. For all, the phenotypic penetrance is high, ~95%. Similar distributions were also seen for TGN46, GCC88, and GS27 (data not shown). The distributions of EEA1, an endosomal marker (data not shown), and LAMP2, a late endosomal/lysosomal marker (Figure 3C), showed little change with ZW10 knockdown, providing a strong indication that the effects were Golgi specific. We conclude that ZW10 depletion produces a general disruption of the Golgi ribbon without any obvious dissociation of kinesin or golgins from Golgi membranes. As shown in Figure 2B, siRab6 treatment produced little change in the Golgi ribbon for all the tested Golgi markers, including endogenous GalT, p115, and GM130. Because the antibody to endogenous Rab6 works well by immunofluorescence, we were also able to score the incidence of siRab6-treated cells that displayed minimal to no detectable Rab6 fluorescence, and we found that Rab6 was knocked down in 96% of the cells. Based on the observed, fragmented, Golgi ribbon phenotype with ZW10 depletion, we conclude that expression of ZW10 is essential for normal Golgi homeostasis.

Organelle-associated Motors Seem to Function in ZW10-depleted HeLa Cells

Varma *et al*. (2006) report that ZW10 depletion in COS cells scatters Golgi ribbon elements about the cytoplasm rather than producing a central cluster of Golgi elements. These authors attribute this to decreased dynein recruitment to Golgi membranes, as assayed in HeLa cells. The overall organization of the Golgi ribbon is known to reflect a balance between inward-directed motors of the dynein class traveling toward the minus end of microtubules and outward directed motors of the kinesin class traveling toward the plus-end of microtubules (Burkhardt *et al*., 1997). As noted here, we found normal association of kinesin with the Golgi apparatus in siZW10(102)-treated HeLa cells (Figure 2A).

We tested motor function in siZW10(102)-treated HeLa cells under several conditions and in several ways. Dynein is known to be involved in the transport to the Golgi of COPII-derived vesicles that bud from the ER. Importantly, we found that transport of tsO45-G protein to the centrally clustered Golgi elements in siZW10(102)-treated cells occurred within a normal, 30-min time frame. As shown in Figure 3A, GFP-conjugated tsO45-G protein accumulated in the ER at nonpermissive temperature and then was transported to the central cluster of Golgi elements in siZW10(102)-treated cells (n = 8 of 8 cells). Furthermore, as

Figure 1 (facing page). Treatment of HeLa cells with siRNAs directed against ZW10 or Rab6 effectively depleted each with little effect on the processing of LAMP2, even though the organization of the Golgi ribbon was affected. HeLa cells stably expressing GalNAcT2-GFP were transfected with either scrambled siRNA (control), siZW10(102), or siRab6(554) at a concentration of 200 nM in the absence of fetal bovine serum for 4 h and then cultured for 72 h. (A) Western blotting using affinity-purified antibodies to human ZW10 showed extensive knockdown of ZW10 relative to GAPDH as control. Similarly, Rab6 was extensively depleted. Under these conditions, there was no detectable decrease in the extensive Golgi glycosylation of LAMP2, and, in Rab6 siRNA treatment, a small increase in glycosylation as indicated by decreased mobility. (B–D) Fluorescence characterization of the distribution of GalNAcT2-GFP (green) indicated that siZW10 and siRab6 treatment had contrasting effects on the organization of the Golgi ribbon with little, if any, effect on the arrangement of microtubules (MT; white) or general cell shape. Asterisk in C, siZW10(102) marks an example of the occasional nondisrupted Golgi apparatus (~5%) seen in cells treated with siRNA directed against ZW10. (E and F) Normal distribution of ER exit sites (Sec13a; white) in HeLa cells treated with siScrambled (E) or siZW10(102) (F) siRNAs for 72 h and stained for endogenous GalT (red). Images shown in B–F are all maximum intensity projections of confocal image stacks through the full cell depth. These images were taken with a 63×/1.40 numerical aperture objective. (G and H) Photobleaching and quantification was done as described under *Materials and Methods* at room temperature. Arrowheads in G point to ~1-μm^2 areas bleached and quantified as illustrated in H for several examples.

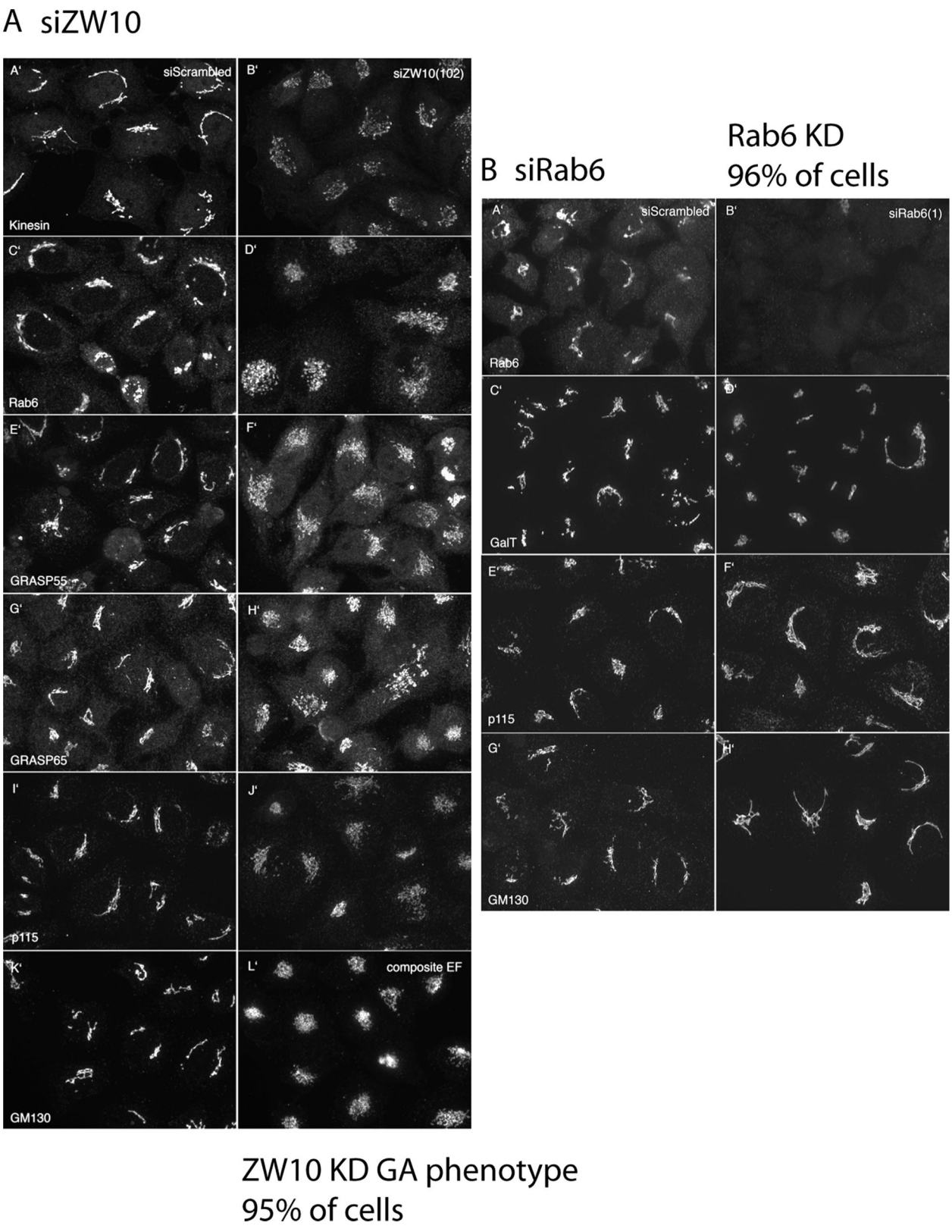

Figure 2. Effect of siRNAs directed against ZW10 and Rab6 on the distribution of a wide range of Golgi proteins. (A and B) Wild-type HeLa cells were siRNA treated for 72 h as described in the legend to Figure 1, and then they were stained for various endogenous Golgi-associated proteins (Kinesin, Rab6, GRASP55, GRASP65, p115, and GM130. GalT). Micrographs taken with a 63×/1.4 numerical aperture objective under identical exposure conditions for both scrambled siRNA-treated cells and cells treated with either siZW10(102) or Rab6(554). All micrographs shown in A and B are single plane projections of full-cell, confocal image stacks.

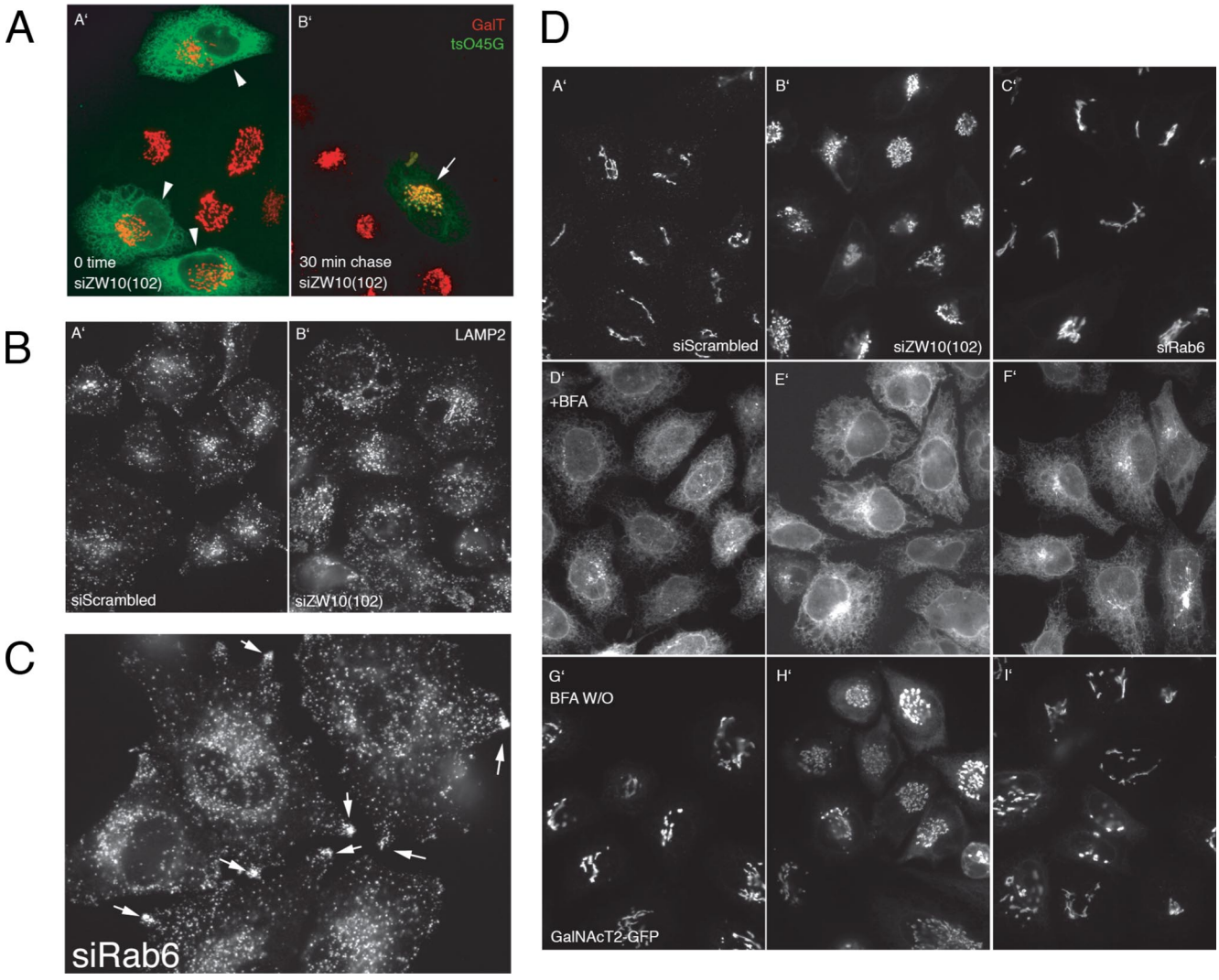

Figure 3. siRNAs directed against ZW10 had little, if any, effect on minus- and plus-end–directed movement of Golgi elements or late endosomes/lysosomes; in contrast, siRNAs directed against Rab6 induced plus-end accumulation of late endosomes/lysosomes at the cell periphery. siRNA treatments were for 72 h as described in the legend to Figure 1. All images shown are full-cell confocal image projections into a single plane. (A) A′ and B′, transport (minus-end–directed transport) of tsO45G-GFP protein from ER to clustered Golgi elements in siZW10(102) occurred in the normal 30-min time frame. Cells are stained for GalT (red). (B) A′ and B′, siZW10(201) treatment for 72 h had had minor effects on the distribution of LAMP2, a late endosomal/lysosome marker. (C) Treatment of GalNAcT2-GFP HeLa cells were siRab6(554) dispersed LAMP2 to toward the cell periphery. Arrows point to LAMP2 concentrations in cell tips. (D) A′–I′, the Golgi apparatus in both siZW10(102)- and siRab6(554)-treated cells is sensitive to BFA (plus-end–directed transport) and Golgi reassembly occurred after BFA washout and transport (minus-end–directed transport) of GalNAcT2-GFP from the ER.

shown in Figure 3B, the effect of ZW10 depletion on the localization of lysosomes and late endosomes was minor, as indicated by the distribution and intensity of LAMP2 staining, which was only slightly more dispersed than in control cells. In fact, and interestingly, Rab6 knockdown had an effect on the distribution of LAMP2. Rab6 is known to recruit dynein to membranes (Short *et al*., 2002; Matanis *et al*., 2003), and it must interact with endocytic structures based on its role in endosome to Golgi trafficking (Mallard *et al*., 2002). In siRab6 cells, the late endosome/lysosome distribution was more scattered and distinct peripheral accumulations of LAMP2-positive late endosomes/lysosomes were apparent (Figure 3C, arrowheads). However, as shown above, Rab6 depletion does not scatter Golgi elements about the cytoplasm; we suggest that this is because Golgi adherence is still predominant.

As an additional test for motor activity in siZW10(102)-treated cells, we incubated HeLa cells with BFA. BFA has long been known to disperse Golgi proteins into the ER in a kinesin-dependent process (Lippincott-Schwartz *et al*., 1995). As shown in Figure 3D, the Golgi apparatus, GalNAcT2 marker, was susceptible to BFA dispersal whether it be control (mock-treated or scrambled siRNA treated), siZW10(102), or siRab6-treated cells. With a 30-min BFA treatment, all showed substantial ER accumulation of GalNAcT2 as indicated by nuclear rim fluorescence and a web-like cytoplasmic distribution. For siZW10-treated cells, there was somewhat more juxtanuclear fluorescence observed than in control cells. This delay was more accentuated at shorter time points (data not shown). In Rab6-depleted cells, there was more residual juxtanuclear Golgi fluorescence, consistent with the previous results, by using dominant-

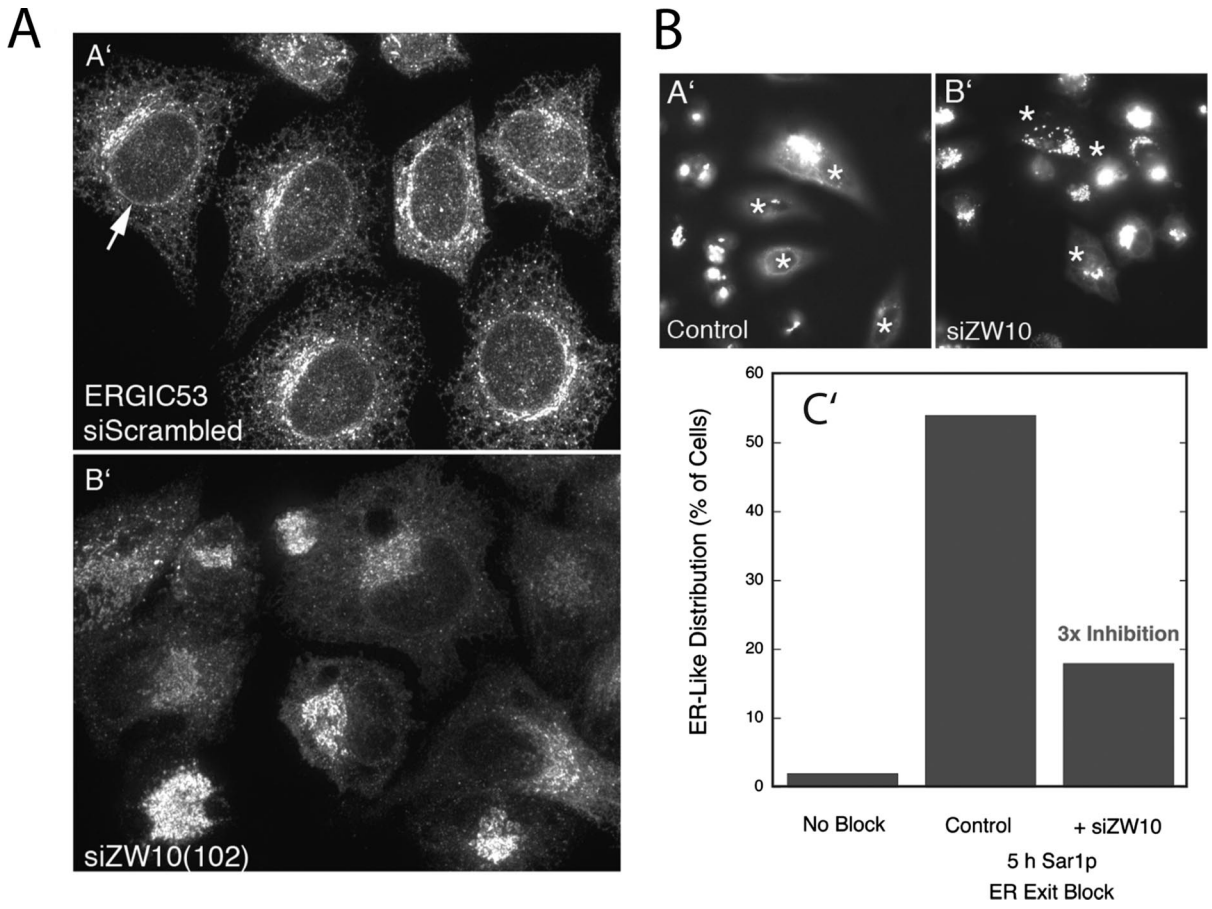

Figure 4. siRNAs directed against ZW10 inhibited the cycling of ERGIC53 and Golgi enzymes to the ER. (A) Effect of 200 nM siZW10(102) treatment for 72 h on the distribution of ERGIC53. siScrambled (A′) and siZW10(102) (B′), 72 h. Full-cell confocal image projections into a single plan. (B) Effect of ZW10 knockdown on the constitutive recycling of a Golgi enzyme, GalNAcT2, to the ER as revealed by a Sar1p ER exit block. HeLa cells stably expressing GalNAcT2-GFP were treated with 200 nM ZW10(102) siRNA for 70 h, two cycles of transfection. Control and siZW10 cells were microinjected with a pCMUIV plasmid encoding GDP-restricted Sar1p. Five hours later, cells were fixed, and the distribution of GalNAcT2 was scored on an individual cell basis. In absence of any block, ER-like distribution of GalNAcT2 was rare (no block). In the siZW10 cells, there was a 3 times inhibition. Asterisks in A′ (control) and B′ (siZW10) mark examples of injected cells. Widefield micrographs.

negative expression of GDP-restricted Rab6a (Jiang and Storrie, 2005). Dispersal to the ER with a 30-min BFA is within the normal kinetic range indicating that kinesin activity was high under all conditions. We then tested for Golgi reformation after BFA washout, a dynein-dependent process. At 2 h after washout, there was substantial, but not complete, reformation of Golgi ribbons in control and siRab6-treated cells. In siZW10(102)-treated cells, the reformation resulted in centrally clustered Golgi elements, indicating that ZW10 is required for the formation of a normal Golgi ribbon. In sum, the BFA experiments indicate that ZW10 depletion does not have substantial functional effects on either plus- or minus-end–directed motor activity related to general juxtanuclear Golgi positioning and assembly. Furthermore, the results observed are mutually consistent; substantial ER-to-Golgi transport was observed both during Golgi reassembly after BFA washout and in tsO45-G protein transport from the ER to clustered Golgi elements.

ZW10 Depletion Inhibits Recycling between the Intermediate Compartment/ERGIC and ER and Golgi Cisternae and ER

To test further the functional consequences of ZW10 depletion, we asked whether protein cycling between the intermediate compartment/ERGIC/Golgi apparatus and ER was affected. ERGIC53 is a lectin needed for the efficient ER exit of certain proteins. It cycles between the ER and intermediate compartment/ERGIC/*cis* Golgi network in a COPI coat protein-dependent manner. In control cells, much of ERGIC53 was located in the ER, and some was concentrated perinuclearly (Figure 4A). In siZW10(102)-treated cells, there was little, to no, detectable ER signal, and ERGIC53 fluorescence was concentrated in centrally clustered elements (Figure 4A). These results suggest that anterograde cycling of ERGIC53 from the ER to ERCIG/Golgi apparatus is still normal, but retrograde cycling must be inhibited in ZW10-depleted cells. Therefore, ERGIC53 accumulates in the ERGIC/Golgi apparatus. In the presence of an ER exit block, Golgi enzymes accumulate gradually in the ER in a COPI coat protein-independent manner (for a recent review, see Storrie, 2005a). As shown in Figure 4B (asterisks indicate cells microinjected to block ER exit), this gradual accumulation was inhibited in siZW10(102) cells, indicating that cisternal Golgi-to-ER cycling was affected in this short-term, 5-h experiment. Note that in this experiment, the extent of cells showing a predominantly ER distribution of Golgi enzyme was ~55% in the control; this is less than we have reported previously (e.g., Storrie *et al*., 1998; Miles *et al*.,

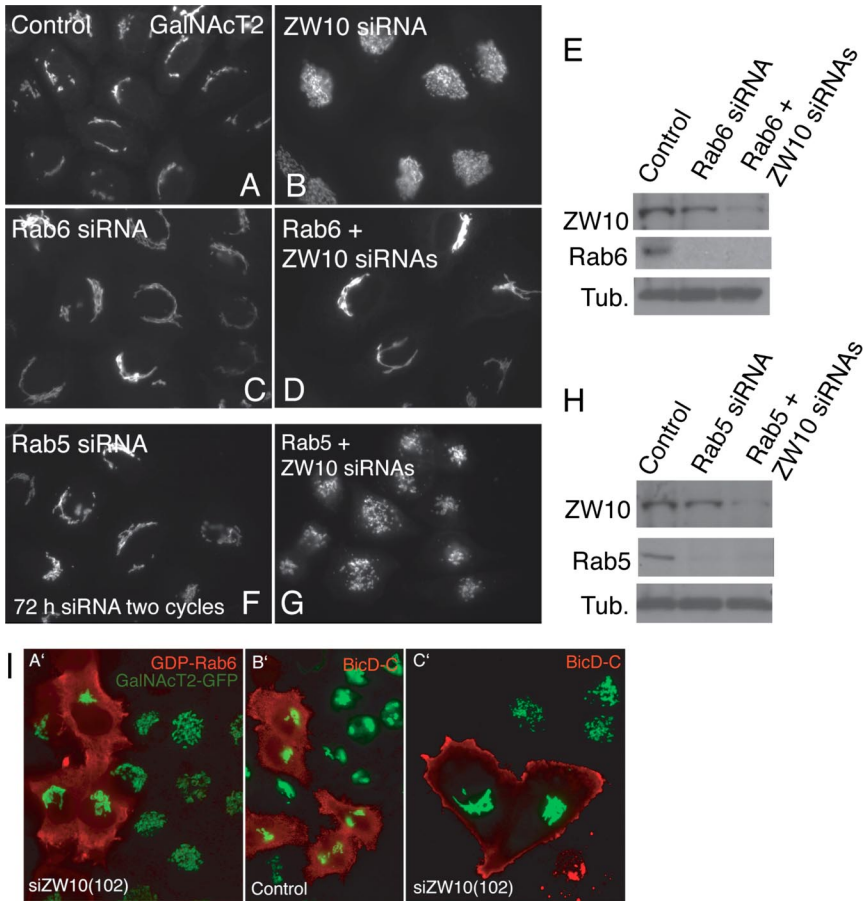

Figure 5. Rab6 depletion, GDP-Rab6a overexpression, or overexpression of BicD C-fragment, a Rab6 effector blocker, inhibit ZW10(102) siRNA-induced dispersal of the Golgi apparatus. (A–D) Cells double-treated with Rab6 + ZW10(102) siRNAs show compact Golgi phenotype. HeLa cells stably expressing GalNAcT2-GFP were mock (scrambled siRNA) (A) or ZW10(102) (B), Rab6 (C), and double (Rab6 + ZW10) (D) siRNA treated for 72 h and then fixed. Widefield images. (E) Total cell lysates from A to D were immunoblotted with anti-ZW10 (top row), anti-Rab 6 (middle row), and anti-tubulin (bottom row) antibodies. (F–H) Rab5 siRNA knockdown does not interfere with ZW10(102) siRNA-induced unraveling of Golgi. HeLa cells stably expressing GalNAcT2-GFP were Rab5 (F) or double (Rab5 + ZW10) (G) siRNA treated. (H) Total cell lysates from F and G were immunoblotted with anti-ZW10, anti-Rab5, and anti-tubulin as a loading control. (I) A′, GDP-Rab6a overexpression inhibited display of the siZW10 Golgi phenotype. GalNAcT2-GFP HeLa cells were transfected with ZW10 siRNA for 57 h, and then plasmids encoding GDP-Rab6 (100 ng/μl) were microinjected into cell nuclei. Six hours later, cells were fixed and stained with anti-Rab6 antibody (red). In the injected cells (red), the Golgi apparatus has a compact, juxtanuclear distribution. Strong inhibition of the ZW10 knockdown phenotype was seen in 60% of the microinjected cells. Widefield images. B′ and C′, expression of BicD C-fragment inhibits Golgi dispersal in response to ZW10 depletion. B′, control GalNAcT2-GFP HeLa cells were microinjected with plasmids (80 ng of DNA/μl stock concentration) encoding BicD C-fragment (myc tagged), and after a 24-h expression period they were myc stained (red). Expression of BicD C-fragment had no effect on the organization of the Golgi ribbon. C′, HeLa cells stably expressing GalNAcT2-GFP were incubated for 48 h after transfection with ZW10(102) siRNA. At 24 h post-siRNA transfection, cells were microinjected with plasmids (60–200 ng DNA/μl encoding BicD C-fragment; myc tagged). At the end of the 24-h expression period, cells were fixed and stained with anti-myc antibody to identify BicD-C–positive cells (red). BicD-C cells, 50% incidence, frequently showed a compact, juxtanuclear Golgi apparatus in comparison with the unraveled Golgi apparatus normally seen with ZW10 knockdown. Widefield images.

2001). These observations are consistent with ZW10 having a role in retrograde membrane trafficking, as might be expected for a ZW10/RINT-1 complex that interacts with the ER target membrane-associated SNARE syntaxin 18 (Hirose *et al*., 2004; Arasaki *et al*., 2006) and the previously cited homologies of these components to a retrograde tether complex in yeast. Some of the effects of ZW10 loss-of-function on anterograde transport reported by Hirose *et al*. (2004) may be the indirect consequence of an inhibition of retrograde trafficking.

In total, our results suggest that ZW10 depletion has at least two selective effects on Golgi apparatus organization and function: 1) an apparent decrease in adherence of the Golgi ribbon/intermediate compartment/ERGIC that leads to its now being a central cluster of Golgi elements; and 2) an inhibition of retrograde trafficking to the ER. Further mechanistic data are required to know whether these two outcomes are independent of one another or whether one might be the indirect consequence of the other. Our results are consistent with the possibility that ZW10 may play a tethering role in Golgi-to-ER trafficking.

Rab6 Loss-of-Function Suppresses ZW10/RINT-1 Knockdown-induced Golgi Fragmentation

Rab6 is a Golgi-associated regulator of COPI-independent, retrograde trafficking between the Golgi and ER; overexpression of Rab6 has been long known to promote Golgi-to-ER trafficking (Martinez *et al*., 1997) and dominant-negative GDP-Rab6 to inhibit (Girod *et al*., 1999). If, as may be hypothesized, the disruption of the Golgi ribbon with ZW10 depletion is a consequence of decreased tethering activity at the ER, then Rab6 loss-of-function might well suppress the observed Golgi disruption. To test this possibility, we assessed Golgi organization in epistatic loss-of-function experiments in which ZW10 (or its binding partner RINT-1) and Rab6 were simultaneously knocked down. As shown in Figure 5, A to E, if both Rab6 and ZW10 were depleted, the Golgi phenotype displayed was that of Rab6 knockdown, i.e., a relatively continuous Golgi ribbon rather than a centrally clustered cloud of Golgi elements as expected for ZW10 depletion alone. The Rab6 effect was specific as indicated by the lack of a co-knockdown effect when Rab5 was depleted rather than Rab6. Under these conditions, the Golgi phenotype is the same as that produced by ZW10 knockdown (Figure 5, F–H). As additional tests for the functional need for Rab6 in Golgi disruption, we overexpressed either the dominant-negative Rab6 mutant GDP-restricted Rab6a or the dominant-negative Rab6 effector BicD C-fragment in control and siZW10(102) cells. Both may have a dominant-negative effect on the development of the ZW10 knockdown phenotype; GDP-restricted Rab6a competes for the guanine

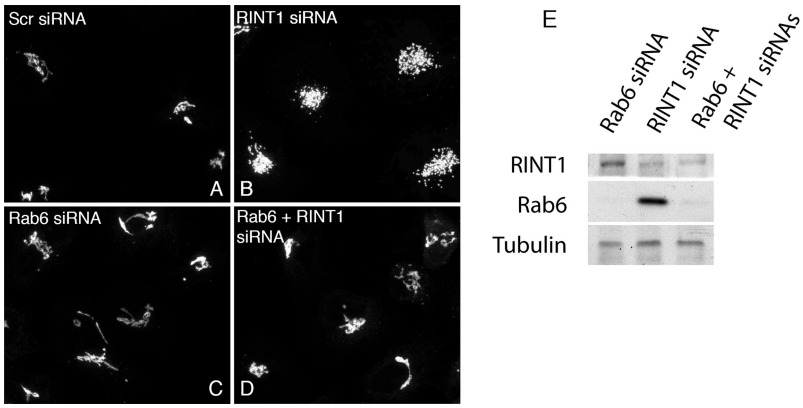

Figure 6. Rab6 depletion inhibits RINT-1 siRNA-induced dispersal of the Golgi apparatus. (A–D) Cell double-treated with Rab6 + RINT-1 siRNAs shows compact Golgi phenotype. HeLa cells stably expressing GalNAcT2-GFP were control (scrambled siRNA) (A) or RINT-1 (B), Rab6 (C), and double (Rab6 + RINT-1) (D) siRNA treated for 72 h and then fixed. Micrographs are maximum intensity projection of confocal image stacks. (E) Total cell lysates were immunoblotted with anti-RINT-1 (top row), anti-Rab6 (middle row), and anti-tubulin (bottom row) antibodies.

nucleotide exchange factor used by both Rab6a and Rab6a′ (Jiang and Storrie, 2005) and the BicD C fragment inhibits Rab6 dependent recruitment of dynein to Golgi membranes (Short *et al.*, 2002; Matanis *et al.*, 2003). As shown in Figure 5I, expression of either GDP-Rab6a or the mutant Rab6 effector, BicD C fragment inhibited the development of the ZW10 Golgi phenotype strongly. BicD C fragment when expressed alone had little, if any, effect on Golgi organization. These data reinforce the conclusion from siRNA double-knockdown experiments that Rab6 acts to initiate a pathway that subsequently involves ZW10 and that is essential to normal Golgi homeostasis. Moreover, the data indicate Rab6 acts through the Rab6 effector BicD and hence through dynein. As a further test that a significant functional role of ZW10 in normal Golgi homeostasis relates to its formation of a complex with RINT-1, we performed epistatic experiments in which RINT-1 and Rab6 were simultaneously knocked down. As shown in Figure 6, knockdown of RINT-1 produced a central cluster of Golgi elements that closely resembled that produced by ZW10 knockdown. Importantly, codepletion of Rab6 and RINT-1 resulted in a Rab6 phenotype, a relatively compact Golgi ribbon.

We conclude that ZW10/RINT-1 has a mechanistic role in stabilizing the Golgi ribbon against a Rab-dependent, dynein-dependent dispersal. In stating this, we also conclude that Rab6 must be acting as a distal, upstream protein from the ZW10/RINT-1 complex. Under normal conditions, the expression of ZW10/RINT-1 and Rab6 are balanced and the Golgi apparatus is organized into a centrally located ribbon.

Rab6 Loss-of-Function Suppresses COG Complex, but Not p115, Knockdown-induced Golgi Disruption

ZW10/RINT-1 is an example of a potential, retrograde, tether complex in Golgi-to-ER trafficking. COG is a known tether complex of eight proteins that is implicated in intra-Golgi retrograde trafficking between the *trans*- and *medial*/*cis*-cisternae (for review, see Ungar *et al.*, 2006). Rab6 may be important in more than one retrograde trafficking pathway. Before investigating this possibility through epistatic knockdown experiments and antibody perturbation of COG function, we asked whether ZW10 and COG acted separately in maintaining normal Golgi homeostasis. We compared the distribution of the Golgi apparatus in HeLa cells treated with COG3 siRNA alone or together with ZW10 siRNA. As shown in Figure 7 and as expected from previous results (Zolov and Lupashin, 2005), COG3 siRNA treatment produced a fragmented Golgi apparatus as highlighted by the yellow fluorescent, perinuclear patches positive for GM130 (green) and *N*-acetylglucosaminyltransferase I (red; GlcNAcT1), a *medial*-Golgi enzyme, together with scattered cytoplasmic vesicles (red) positive for GlcNAcT1. GlcNAcT1 is used in these experiments because it is a very effective marker for COG knockdown-dependent Golgi vesiculation (Zolov and Lupashin, 2005). In a double siRNA experiment, the Golgi phenotype observed displayed fragments showing some central clustering, a common result to COG3p and ZW10 depletion, and scattered vesicles as indicated by the diffuse cytoplasmic fluorescence for GlcNAcT1, a result seen only with COG3p depletion. The overall phenotype observed could only be produced if ZW10 depletion did not interfere with the effect of COG3p depletion on intra-Golgi vesicular trafficking, suggesting that there is no epistatic relationship between COG and ZW10.

Next, we tested the epistatic relationship of Rab6 to COG. In addition to RNAi, we used an inhibitory antibody approach. As shown by the Lupashin laboratory (Suvorova *et al.*, 2002), COG function can be disrupted by microinjection

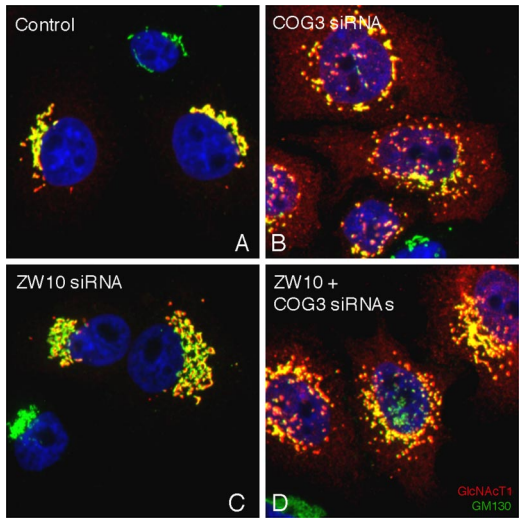

Figure 7. HeLa cells double-treated with COG3 and ZW10 siRNAs display a phenotype that shows vesicular accumulation of GlcNAcT1 as observed with COG3 siRNA treatment. HeLa cells stably expressing GlcNAcT1-myc (red channel) were mock (control, A) or COG3 (B). ZW10 (C) and double (ZW10 + COG3) (D) siRNA treated for 72 h, 100 nM individual duplex siRNA concentration, fixed, and stained with anti-myc antibody, anti-GM130 (green channel); and DNA (DAPI, blue channel). Image stacks were taken with the CARV II spinning disk confocal accessory and projected into a single XY plane.

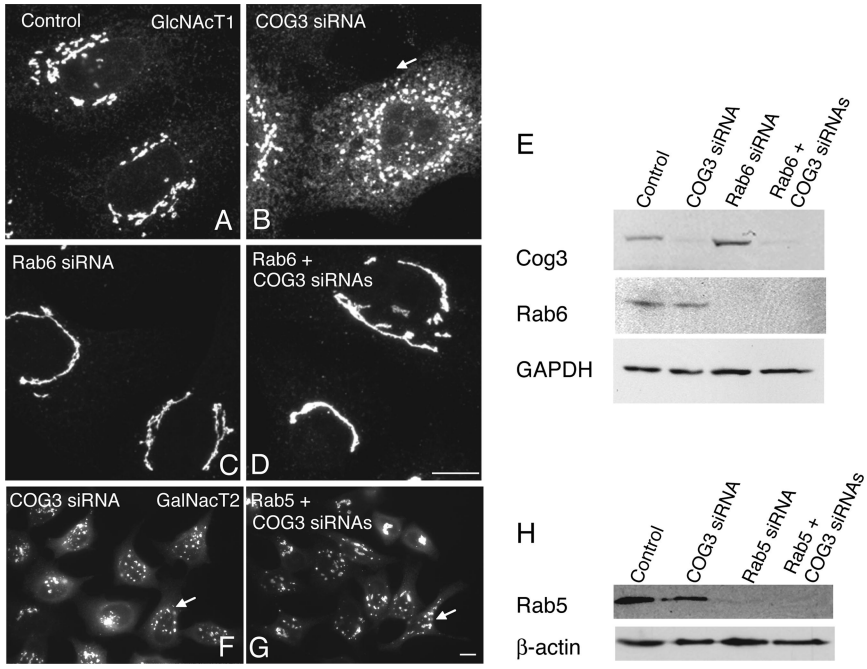

Figure 8. Rab6 depletion inhibits COG3 siRNA-induced fragmentation of Golgi and accumulation of GlcNAcT1 in vesicles. (A–D) Cells double-treated with Rab6 + COG3 siRNAs show compact Golgi phenotype. HeLa cells stably expressing GlcNAcT1-myc were mock (control) (A) or COG3 (B), Rab6 (C), and double (Rab6 + COG3) (D) siRNA treated for 72 h, fixed, and stained with anti-myc antibody. Myc signal was collected as confocal image stacks by using a CARV II confocal accessory. (E) Total cell lysates from A to D were immunoblotted with anti-Cog3 (top row), anti-Rab 6 (middle row), and anti-GAPDH (bottom row) antibodies. (F–H) Rab5 siRNA knockdown does not interfere with COG3 siRNA-induced fragmentation of Golgi. HeLa cells stably expressing GalNAcT2-GFP were COG3 (F) or double (Rab5/COG3) (G) siRNA treated. (H) Total cell lysates from F and G were immunoblotted with anti-Rab5 and anti-β-actin as a loading control. Efficiency of knockdown was ~90%. Widefield images. Arrows indicate fragmented Golgi apparatus. Bar, 10 μm.

of antibodies directed against Cog3. Antibody disruption in comparison with RNA interference is a rapid and complementary approach that produces an acute, short-term phenotype in 4 h. As shown in Figures 8 and 9, siRab6 treatment suppressed the Golgi fragmentation and vesiculation induced by either siRNA depletion of COG3p or inhibitory antibodies directed against COG3p. The loss-of-function of two proteins produced a normal Golgi ribbon, suggesting that Rab6 through effectors initiates the formation of retrograde intra-Golgi intermediates whose consumption is COG dependent. The COG complex is required for intra-Golgi trafficking and ZW10 is predominantly an ER protein in interphase HeLa cells. Probably, Rab6 recruits different effectors relative to COG and ZW10. As a test of this, we asked whether overexpression of BicD C-fragment during a COG3p knockdown would inhibit the development of the COG3p knockdown Golgi phenotype. We found that it did not (data not shown), indicating a role for different Rab6 effectors in each pathway. Finally, we tested in epistatic siRNA experiments whether Rab6 acted upstream of p115 in HeLa cells. As shown in Figure 10, codepletion of Rab6 and p115 resulted in the p115 phenotype of a fragmented Golgi ribbon with some accumulation of GalNAcT2 in the ER. In sum, the data indicate that Rab6 acts to initiate vesicle formation relative to COG, a putative tether complex, in retrograde trafficking within the Golgi cisternal stack, but has little, if any, relationship to p115, a tether thought to be active in anterograde membrane trafficking to Golgi apparatus.

In sum, Rab6 regulates ZW10/RINT-1- and COG-dependent Golgi trafficking/homeostasis, but not p115-dependent Golgi trafficking/homeostasis.

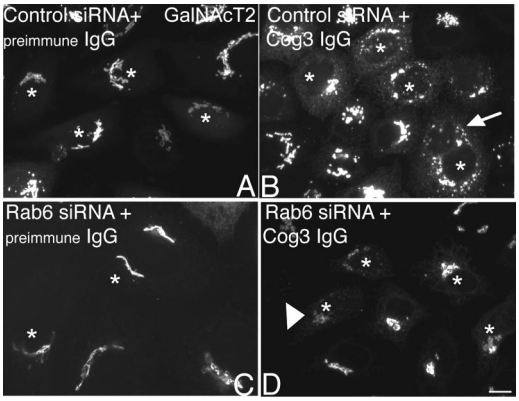

Figure 9. Rab6 knockdown reduces Golgi fragmentation caused by microinjection of Cog3 antibody. HeLa cells stably expressing GalNAcT2-GFP were mock (A and B) or Rab6 (C and D) siRNA treated for 72 h. Cells were microinjected with affinity-purified anti-Cog3 (A and C) or preimmune (B and D) antibodies and fixed 4 h after microinjection. GFP signal was collected as confocal image stacks by using a CARV II confocal accessory. Arrow, fragmented Golgi; arrowhead, compact Golgi; asterisk, injected cells. Bar, 10 μm.

DISCUSSION

We started from the working hypothesis that the organization of the mammalian Golgi apparatus into a juxtanuclear ribbon is a balance between membrane trafficking/transport and adherence of Golgi stacks, all of which are under the control of members of the Rab family of small GTPases. We chose to concentrate on the interrelationship between Rab6, a small GTPase long known to promote Golgi-to-ER trafficking (Martinez *et al.*, 1997; Girod *et al.*, 1999; White *et al.*, 1999) and the most abundant Golgi cisternal Rab (Gilchrist *et al.*, 2006), and ZW10. In mitotic cells, ZW10 is a mitotic checkpoint protein (Karess, 2005). In interphase cells, ZW10 interacts through RINT-1 with the ER SNARE syntaxin 18, and it is part of a potential tether complex for Golgi/ER trafficking (see Supplemental Figures in Andag and Schmitt, 2003; Hirose *et al.*, 2004; Arasaki *et al.*, 2006). Interactions with dynein have also been noted (Varma *et al.*, 2006). Results were contrasted with those characterizing the interrelationship between Rab6 and the COG complex and p115, well-established, putative Golgi tether components for intra-Golgi retrograde trafficking and anterograde trafficking between the ER and

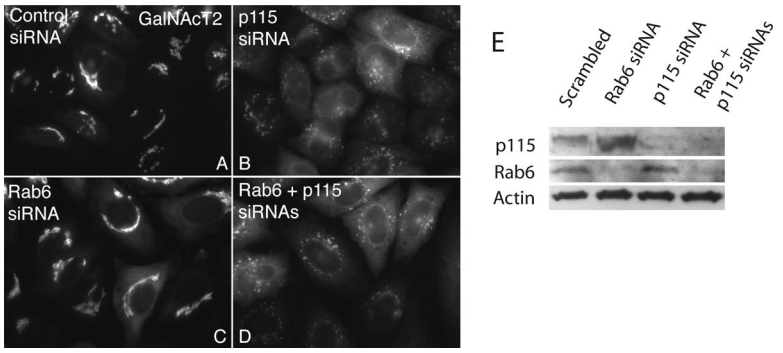

Figure 10. Rab6 knockdown fails to inhibit Golgi fragmentation in response to p115 depletion. HeLa cells stably expressing GalNAcT2-GFP were treated for 72 h with control scrambled siRNA (A), p115 siRNA (B), Rab6 siRNA (C), or p115 + Rab6 siRNAs (D). Widefield images. (E) Immunoblot showing that p115 and Rab6 are appropriately knocked down.

Golgi apparatus, respectively. Our results show that Rab6 is required for Golgi ribbon fragmentation in response to ZW10/RINT-1 or COG depletion, but not p115 depletion. Both ZW10/RINT-1- and COG-dependent Golgi membrane trafficking were Rab6 regulated. To the best of our knowledge, this is the first evidence that a Rab protein has a role in regulating Golgi membrane trafficking and homeostasis through affecting two separate and what must be distal protein complexes: ZW10/RINT-1 and COG, respectively.

The disrupted Golgi phenotype that we observed in ZW10-depleted cells showed little, if any, correlation with altered motor protein activity, and, in fact, depletion-dependent disruption of the Golgi ribbon was inhibited by a protein fragment of a bridging protein between Rab6 and dynein/dynactin, BicD. The organization of microtubules was normal in distribution in ZW10-depleted cells as was the distribution of ER exit sites. Several functional tests of motor activity in ZW10 knockdown cells showed motor-dependent membrane transport was within the normal time frames. However, consistent with the observations of Varma *et al*. (2006) that ZW10 can recruit dynein to membranes, we observed that lysosomes/late endosomes were more dispersed in ZW10-depleted cells; dynein is required for the juxtanuclear clustering of these organelles (Burkhardt *et al*., 1997). Multiple lines of evidence indicate that ZW10 depletion has a distinct phenotypic effect on the Golgi apparatus that manifests itself as an inhibition of Golgi-to-ER protein cycling. In ZW10 knockdown cells displaying the characteristic clustered cloud of Golgi elements, the recycling of ERGIC53 to the ER was strongly inhibited as indicated by the accumulation of ERGIC53 in a greatly expanded, presumably *cis*-Golgi/intermediate compartment as seen by fluorescence microscopy. Moreover, when a short-term ER exit block was used to trap cycling Golgi enzymes in the ER, significant inhibition of GalNAcT2 accumulation in the ER was seen in ZW10-depleted cells. We suggest that the failure of Arasaki *et al*. (2006) to observe a ZW10 knockdown-dependent inhibition of Golgi-to-ER recycling is an outcome of the long end time point of their experiments, 17 h. We used a 5-h block.

Most likely the inhibitory effects on retrograde recycling from the Golgi to the ER relate mechanistically to ZW10's complexing with RINT-1 and the ER SNARE syntaxin 18 (Hirose *et al*., 2004; Arasaki *et al*., 2006). The fact that both ERGIC53 and GalNAcT2 recycling were inhibited is significant, because one process is thought to be a COPI coat protein-dependent process and the other to be a COPI coat protein-independent process (for reviews, see Storrie *et al*., 2000; Storrie, 2005). Conceivably, the two processes converge upon the same SNARE proteins at the ER for membrane fusion. Importantly, co-siRNA depletion for Rab6 and RINT-1 suppresses the ZW10 knockdown-like Golgi phenotype seen with RINT-1 depletion. This result is significant also as a control that the siRNA effects with ZW10 depletion are specific for ZW10/RINT-1, a known interacting protein complex in interphase cells (Hirose *et al*., 2004; Arasaki *et al*., 2006) rather than being an off-target effect of the siRNA treatment. We note that the effects of ZW10 loss-of-function reported previously by Hirose *et al*. (2004) on anterograde trafficking could be an indirect outcome of inhibited recycling of Golgi components.

The relationship of Rab6 to ZW10 is protein specific. Epistatic knockdown of Rab5, an endosomal Rab, failed to inhibit ZW10 depletion induced Golgi dispersal and overexpression of GDP-Rab6, the inactive form of Rab6, inhibited ZW10 depletion induced Golgi dispersal. Furthermore, the inhibition by BicD-C fragment cited above is another indicator of specificity as BicD is a Rab6 effector. Codepletion of Rab6 and Rab41, a second Golgi Rab, failed to inhibit the Golgi dispersal induced by Rab41 depletion (Storrie, unpublished data). We note that in our work, we deliberately used reagents that affect both Rab6a and Rab6a′, the common isoforms of Rab6. In preliminary experiments, we find that treatment of HeLa cells with siRNAs directed specifically against Rab6a inhibit Golgi unraveling and fragmentation in response to ZW10 or COG depletion (Sun, Shestakova, and Storrie, unpublished data). Whether both isoforms of Rab6 are functionally relevant will require detailed experimentation. In addition, we find that treatment of HeLa cells with siRNAs directed against a medial Rab can also inhibit Rab6 promoted Golgi trafficking and ZW10 depletion-dependent Golgi dispersal (Sun, Starr, and Storrie, unpublished observations), providing an additional line of evidence that Rab6 is acting to initiate a process in which ZW10/RINT-1 are downstream components.

The Rab6 depletion suppressed COG knockdown phenotype was highly Rab specific, because Rab5 depletion had no effect on the COG knockdown phenotype. Rab6 knockdown inhibited COG-dependent Golgi fragmentation whether induced by 72-h COG silencing or acutely by microinjection of COG3p antibodies. Our data strongly indicate that Rab6 does not act in a p115-dependent pathway. From the observations that codepletion of ZW10 and COG had no effect on COG depletion-dependent vesicle accumulation and the differential effect of BicD C-fragment on ZW10- versus COG depletion-induced Golgi disruption, we conclude that ZW10 and COG are involved in separate Golgi trafficking pathways. The COG complex is thought to be a multiprotein tether in COPI coat protein-dependent intra-Golgi recycling of Golgi enzymes (for review, see Ungar *et al*., 2006). The yeast COG complex interacts genetically with at least two different Golgi-localized Rab proteins, Ypt1 and Ypt6 (Whyte and Munro, 2001; Ram *et al*., 2002; Suvorova *et al*., 2002). In mammals, the homologue of Ypt6, Rab6, is concen-

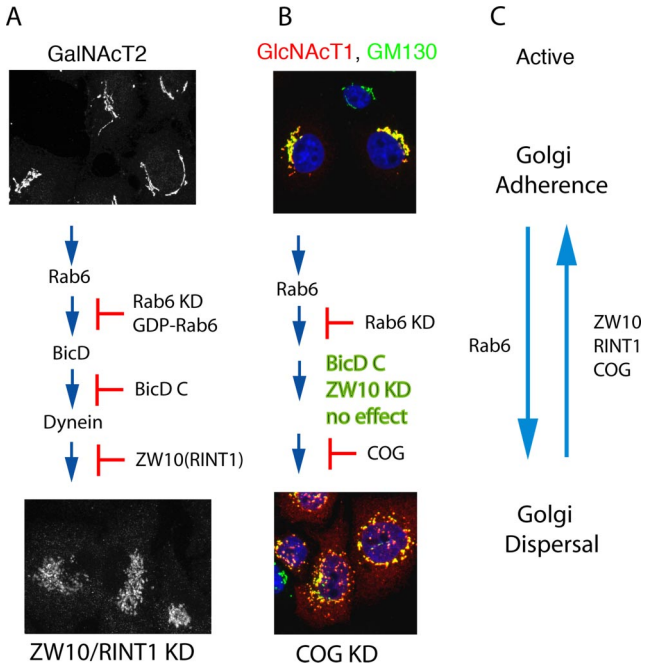

Figure 11. Schematic model of the initiating role of Rab6 in ZW10/RINT-1– and COG-dependent Golgi trafficking pathways necessary for normal Golgi homeostasis. Our data suggest that a role of Rab6 is in the initiation of two Golgi recycling pathways: recycling of Golgi components to the ER in pathway requiring a BicD-dependent motor and ZW10/RINT-1 (A) and intra-Golgi recycling of Golgi enzymes in a COG-dependent pathway (B). Rab6 has no effect on p115 anterograde trafficking. Both pathways are required for normal Golgi homeostasis. (C) Balance of the various proteins relative to Golgi adherence versus dispersal.

trated in the *trans*-Golgi/TGN; hence, it is likely to act at this site in any promotion of retrograde carriers. Probing for the exact functional links between Rab6 and ZW10/RINT-1 and COG complex are now important future questions.

In conclusion, our work strongly indicates that Rab6 acts to initiate two separate Golgi-trafficking pathways important to Golgi trafficking and homeostasis that involve, respectively, ZW10/RINT-1 and the putative COG retrograde tether complex. Furthermore, the data indicate that ZW10/RINT-1 and COG act independently of one another in Golgi homeostasis and function. Importantly, our data suggest that ZW10 has at least two mechanistic roles in Golgi homeostasis, one being in Golgi recycling to the ER and a second in the adherence of the Golgi ribbon; we note that the one may be an indirect consequence of the other. In addition, ZW10 has a role in dynein recruitment with respect to lysosomes/late endosomes. Its role in dynein recruitment with respect to the Golgi apparatus as indicated by the work of Varma *et al*. (2006) may only be revealed with more extensive protein knockdown than achieved in the present study. We suggest that the respective roles of ZW10 in mitotic and interphase cells are determined by the molecular context in which the protein is presented. In conclusion, we summarize diagrammatically the relative roles of Rab6, ZW10/RINT-1, and GOG in Golgi membrane trafficking and homeostasis in Figure 11.

ACKNOWLEDGMENTS

We greatly appreciate the gifts of antibodies and reagents from colleagues. We express our appreciation to Ngozi Wilkins and Alexi Pavliv for expert technical assistance. This work was supported in part by grants from the National Science Foundation (MCB-0549001 to B.S. and MCB-0645163 to V.L.) and the Mizutani Foundation for Glycoscience (to V.L.), and it was initiated with support from the Arkansas Biosciences Institute.

REFERENCES

Allan, B. B., Moyer, B. D., and Balch, W. E. (2000). Rab1 recruitment of p115 into a cis-SNARE complex: programming budding COPII vesicles for fusion. Science *289*, 444–448.

Andag, U., and Schmitt, H. H. (2003). Dsl1p, an essential component of the Golgi-endoplasmic reticulum retrieval system in yeast, uses the same sequence motif to interact with different subunits of the COPI vesicle coat. J. Biol. Chem. *278*, 51722–51734.

Antony, C., Cibert, C., Geraud, G., Santa Maria, A., Maro, B., Mayau, V., and Goud, B. (1992). The small GTP-binding protein rab6p is distributed from medial Golgi to the traan-Golgi network as determined by a confocal microscopic approach. J. Cell Sci. *103*, 785–796.

Arasaki, K., Taniguchi, M., Tani, K., and Tagaya, M. (2006). RINT-1 regulates the localization and entry of ZW10 to the syntaxin 18 complex. Mol. Biol. Cell *17*, 2780–2788.

Burkhardt, J. K., Echeverri, C. J., Nilsson, T., and Vallee, R. B. (1997). Overexpression of the dynamitin (p50) subunit of the dynactin complex disrupts dyein-dependent maintenance of membrane organelle distribution. J. Cell Biol. *139*, 469–484.

Del Nery, E., Miserey-Lenkei, S., Falguieres, T., Nizak, C., Johannes, L., Perez, F., and Goud, B. (2006). Rab6A and Rab6A′ GTPases play non-overlapping roles in membrane trafficking. Traffic *7*, 394–407.

Diao, A., Rahman, D., Pappin, D. J., Lucocq, J., and Lowe, M. (2003). The coiled-coil membrane protein golgin-84 is a novel rab effector required for Golgi ribbon formation. J. Cell Biol. *160*, 201–212.

Gilchrist, A. *et al*. (2006). Quantitative proteomics analysis of the secretory pathway. Cell *127*, 1265–1281.

Girod, A., Storrie, B., Simpson, J. C., Johannes, L., Goud, B., Roberts, L. M., Lord, J. M., Nilsson, T., and Pepperkok, R. (1999). Evidence for a COP-I-independent transport route from the Golgi complex to the endoplasmic reticulum. Nat. Cell Biol. *1*, 423–430.

Hirose, H., Arasaki, K., Dohmae, N., Takio, K., Hatsuzawa, K., Nagahama, M., Tani, K., Yamamoto, A., Tohyama, M., and Tagaya, M. (2004). Implication of ZW10 in membrane trafficking between the endoplasmic reticulum and Golgi. EMBO J. *23*, 1267–1278.

Jiang, S., and Storrie, B. (2005). Cisternal rab proteins regulate Golgi apparatus redistribution in response to hypotonic stress. Mol. Biol. Cell *16*, 2586–2596.

Jiang, S., Rhee, S. W., Gleeson, P. A., and Storrie, B. (2006). Capacity of the Golgi apparatus for cargo transport prior to complete assembly. Mol. Biol. Cell *17*, 4105–4117.

Jordens, I., Marsman, M., Kuijl, C., and Neefjes, J. (2005). Rab proteins, connecting transport and vesicle fusion. Traffic *6*, 1070–1077.

Karess, R. (2005). Rod-Zw10-Zwilch: a key player in the spindle checkpoint. Trends Cell Biol. *15*, 386–392.

Kops, G. J., Kim, Y., Weaver, B. A., Mao, Y., McLeod, I., Yates, J. R. 3rd, Tagaya, M., and Cleveland, D. W. (2005). ZW10 links mitotic checkpoint signaling to the structural kinetochore. J. Cell Biol. *169*, 49–60.

Lee, M. C., Miller, E. A., Goldberg, J., Orci, L., and Schekman, R. (2004). Bi-directional protein transport between the ER and Golgi. Annu. Rev. Cell Dev. Biol. *20*, 87–123.

Lippincott-Schwartz, J., Cole, N. B., Marotta, A., Conrad, P. A., and Bloom, G. S. (1995). Kinesin is the motor for microtubule-mediated Golgi-to-ER membrane traffic. J. Cell Biol. *128*, 293–306.

Lupashin, V., and Sztul, E. (2005). Golgi tethering factors. Biochim. Biophys. Acta-Mol Cell Res. *1744*, 325–339.

Mallard, F. *et al*. (2002). Early/recycling endosomes-to-TGN transport involves two SNARE complexes and a Rab6 isoform. J. Cell Biol. *156*, 653–664.

Matanis, T. *et al*. (2003). Bicaudal-D regulates COPI-independent Golgi-ER transport by recruiting the dynein-dynactin motor complex. Nat. Cell Biol. *4*, 986–992.

Martinez, O., Antony, C., Pehau-Arnaudet, G., Berger, E. G., Salamero, J., and Goud, B. (1997). GTP-bound forms of rab6 induce the redistribution of Golgi proteins into the endoplasmic reticulum. Proc. Natl. Acad. Sci. USA *94*, 1828–1833.

Miles, S., McManus, H., Forsten, K. E., and Storrie, B. (2001). Evidence that the entire Golgi apparatus cycles in interphase HeLa cells: sensitivity of Golgi matrix proteins to an ER exit block. J. Cell Biol. *155*, 543–555.

Nizak, C., Monier, S., del Nery, E., Moutel, S., Goud, B., and Perez, F. (2003). Recombinant antibodies to the small GTPase rab6 as conformation sensors. Science *300*, 984–987.

Puthenveedu, M. A., Bachert, C., Puri, S., Lanni, F., and Linstedt, A. D. (2006). GM130 and GRASP65-dependent lateral cisternal fusion allows uniform Golgi-enzyme distribution. Nat. Cell Biol. *8*, 238–248.

Ram, R. J., Li, B., and Kaiser, C. A. (2002). Identification of sec36p, sec37p, and sec38p: components of yeast complex that contains sec34p and sec35p. Mol. Biol. Cell *13*, 1484–1500.

Rogalski, A. A., Bergmann, J. E., and Singer, S. J. (1984). Effect of microtubule assembly status on the intracellular processing and surface expression of an integral protein of the plasma membrane. J. Cell Biol. *99*, 1101–1109.

Sapperstein, S. K., Walter, D. M., Grosvenor, A. R., Heuser, J. E., and Waters, M. G. (1995). p115 is a general vesicular transport factor related to the yeast endoplasmic reticulum to Golgi transport factor Uso1p. Proc. Natl. Acad. Sci. USA *92*, 522–526.

Satoh, A., Wang, Y., Malsam, J., Beard, M. B., and Warren, G. (2003). Golgin-84 is a rab1 binding partner involved in Golgi structure. Traffic *4*, 153–161.

Shestakova, A., Zolov, S., and Lupashin, V. (2006). COG complex-mediated recycling of Golgi glycosyltransferases is essential for normal protein glycosylation. Traffic *7*, 191–204.

Short, B., Haas, A., and Barr, F. A. (2005). Golgins and GTPases, giving identity and structure to the Golgi apparatus. Biochim. Biophys. Acta *1744*, 383–395.

Short, B., Preisinger, C., Schaletzky, J., Kopajtich, R., and Barr, F. A. (2002). The Rab6 GTPase regulates recruitment of the dynactin complex to Golgi membranes. Curr. Biol. *12*, 1792–1795.

Short, B., Preisinger, C., Korner, R., Kopajtich, R., Byron, O., and Barr, F. A. (2001). A GRASP55-rab2 effector complex linking Golgi structure to membrane traffic. J. Cell Biol. *155*, 877–883.

Shorter, J., and Warren, G. (2002). Golgi architecture and inheritance. Annu. Rev. Cell Dev. Biol. *18*, 379–420.

Sohda, M., Misumi, Y., Yoshimura, S., Nakamura, N., Fusano, T., Sakisaka, S., Ogata, S., Fujimoto, J., Kiyokawa, N., and Ikehara, Y. (2005). Depletion of vesicle-tethering factor p115 causes mini-stacked Golgi fragments with delayed protein transport. Biochem. Biophys. Res. Commun. *338*, 1268–1274.

Starr, D. A., Williams, B. C., Li, Z., Etemad-Moghadam, B., Dawe, R. K., and Goldberg, M. L. (1997). Conservation of the centrosome/kinetochore protein ZW10. J. Cell Biol. *138*, 1289–1301.

Storrie, B. (2005a). Maintenance of Golgi apparatus structure in the face of continuous protein recycling to the endoplasmic reticulum: making ends meet. Int. Rev. Cytol. *244*, 69–94.

Storrie, B. (2005b). Microinjection as a tool to explore small GTPase function. Methods Enzymol. *404*, 26–42.

Storrie, B., Pepperkok, R., and Nilsson, T. (2000). Breaking the COPI monopoly on Golgi recycling. Trends Cell Biol. *10*, 385–391.

Storrie, B., White, J., Rottger, S., Stelzer, E. H., Suganuma, T., and Nilsson, T. (1998). Recycling of Golgi-resident glycosyltransferases through the ER reveals a novel pathway and provides an explanation for nocodazole-induced Golgi scattering. J. Cell Biol. *143*, 1505–1521.

Stroud, W. J., Jiang, S., Jack, G., and Storrie, B. (2003). Persistence of Golgi matrix distribution exhibits the same dependence on Sar1p activity as a Golgi glycosyltransferase. Traffic *4*, 631–641.

Suvorova, E. S., Duden, R., and Lupashin, V. V. (2002). The Sec34/Sec35p complex, a Ypt1p effector required for retrograde intra-Golgi trafficking, interacts with Golgi SNAREs and COPI vesicle coat proteins. J. Cell Biol. *157*, 631–643.

Suvorova, E. S., Kurten, R. C., and Lupashin, V. V. (2001). Identification of a human orthologue of Sec34p as a component of the cis-Golgi vesicle tethering machinery. J. Biol. Chem. *276*, 22810–22818.

Sztul, E., and Lupashin, V. (2006). Role of tethering factors in secretory membrane traffic. Am. J. Physiol. *290*, C11–C26.

Ungar, D., Oka, T., Krieger, M., and Hughson, F. M. (2006). Retrograde transport on the COG railway. Trends Cell Biol. *16*, 113–120.

Varma, D., Dujardin, D. L., Stehman, S. A., and Vallee, R. B. (2006). Role of the kinetochore/cell cycle checkpoint protein ZW10 in interphase cytoplasmic dynein function. J. Cell Biol. *172*, 655–662.

Weide, T., Bayer, M., Koster, M., Siebrasse, J. P., Peters, R., and Barnekow, A. (2001). The Golgi matrix protein GM *130*, a specific interacting partner of the small GTPase rab1b. EMBO Rep. *2*, 336–341.

White, J. *et al*. (1999). Rab6 coordinates a novel Golgi to ER retrograde transport pathway in live cells. J. Cell Biol. *147*, 743–759.

Whyte, J. R., and Munro, S. (2001). The Sec34/35 Golgi transport complex is related to the exocyst, defining a family of complexes involved in multiple steps of membrane traffic. Dev. Cell *1*, 527–537.

Williams, B. C., Karr, T. L., Montgomery, J. M., and Goldberg, M. L. (1992). The *Drosophila* l(1)zw10 gene product, required for accurate mitotic chromosome segregation, is redistributed at anaphase onset. J. Cell Biol. *118*, 759–773.

Young, J., Stauber, T., del Nery, E., Vernos, I., Pepperkok, R., and Nilsson, T. (2005). Regulation of microtubule-dependent recycling at the trans-Golgi network by Rab6A and Rab6A′. Mol. Biol. Cell *16*, 162–177.

Zolov, S. N., and Lupashin, V. V. (2005). Cog3p depletion blocks vesicle-mediated Golgi retrograde trafficking in HeLa cells. J. Cell Biol. *168*, 747–759.